

Carboranes and Baskets from Reaction of B<sub>4</sub>H<sub>10</sub> with Allene

Hasan Sayin and Michael L. McKee\*

Department of Chemistry and Biochemistry, Auburn University, Auburn, Alabama 36849

Received January 16, 2007

The reaction of the boron hydride B<sub>4</sub>H<sub>10</sub> with allene was studied at the CCSD(T)/6-311+G(d)//MP2/6-31G(d) level. The mechanism is surprisingly complex with 44 transition states and several branching points located. The four carboranes and one basket that have been observed experimentally are all connected by pathways that have very similar free energies of activation. In addition, two new structures, a basket (2,4-(CH<sub>2</sub>CH<sub>2</sub>CH<sub>2</sub>)B<sub>4</sub>H<sub>8</sub>, **5a**) and a “classical” structure (1,4-(Me<sub>2</sub>C)bisdiborane, **7**), which might be obtained from the B<sub>4</sub>H<sub>10</sub> + C<sub>3</sub>H<sub>4</sub> reaction under the right conditions (hot/cold, quenched, etc.) have been identified. The first branch point in the reaction is the competition between H<sub>2</sub> elimination from B<sub>4</sub>H<sub>10</sub> ( $\Delta G(298\text{ K}) = 32.2\text{ kcal/mol}$ ) and the hydroboration of allene by B<sub>4</sub>H<sub>10</sub> ( $\Delta G(298\text{ K}) = 31.3\text{ kcal/mol}$ ). The next branch point in the hydroboration mechanism controls the formation of 2,4-(MeCHCH<sub>2</sub>)B<sub>4</sub>H<sub>8</sub> (**1**) ( $\Delta G(298\text{ K}) = 31.5\text{ kcal/mol}$ ) and *arachno*-1,2/*arachno*-1,3-Me<sub>2</sub>-1-CB<sub>4</sub>H<sub>7</sub> (**8** and **8a**) ( $\Delta G(298\text{ K}) = 34.3\text{ kcal/mol}$ ). Another branch point in the H<sub>2</sub>-elimination mechanism controls the formation of 1-Me-2,5- $\mu$ -CH<sub>2</sub>-1-CB<sub>4</sub>H<sub>7</sub> (**29**) ( $\Delta G(298\text{ K}) = 0.1\text{ kcal/mol}$ ) and 2,5- $\mu$ -CHMe-1-CB<sub>4</sub>H<sub>7</sub> (**25/26**) ( $\Delta G(298\text{ K}) = 7.3\text{ kcal/mol}$ ). Formation of 2-Me-2,3-C<sub>2</sub>B<sub>4</sub>H<sub>7</sub>, a carborane observed in the reaction of methylacetylene with B<sub>4</sub>H<sub>10</sub>, is calculated to be blocked by a high barrier for H<sub>2</sub> elimination. All free energies are relative to B<sub>4</sub>H<sub>10</sub> + allene. An interesting reaction step discovered is the “reverse hydroboration step” in which a hydrogen atom is transferred from carbon back to boron, which allows a CH hydrogen to shuttle between the terminal and central carbon of allene.

## Introduction

It is well-known that alkynes, alkenes, and enynes react in the gas phase with boranes such as B<sub>4</sub>H<sub>10</sub>, often producing a surprising mixture of compounds<sup>1–8</sup> in which carbon is incorporated into the clusters to form carboranes and/or a basketlike compound.<sup>9–13</sup> Two hydrocarbon isomers, allene and methylacetylene, react with B<sub>4</sub>H<sub>10</sub> to generate six ob-

serveable products depending on the reaction conditions (Scheme 1). Under “hot/cold” conditions with allene, the basket compound 2,4-(MeCHCH<sub>2</sub>)B<sub>4</sub>H<sub>8</sub> (**1**) is formed, as well as four carboranes. On the other hand, methylacetylene forms two of the same carboranes, as well as 2-Me-2,3-C<sub>2</sub>B<sub>4</sub>H<sub>7</sub> (**34**), a product not detected in the allene + B<sub>4</sub>H<sub>10</sub> reaction.

The reaction of boron hydrides with alkynes and alkenes have complex reaction mechanisms with a number of intermediates of similar energy. In contrast to hydrocarbons, the bonding in the boron hydrides is electron deficient where several bonding patterns may have similar stability. There are many examples of “nonclassical” versus “classical” isomers where the former structures have a greater number of three-center two-electron bonds (3c-2e) while the latter structures have a greater number of 2c-2e bonds with a vacant

\* To whom correspondence should be addressed. E-mail: mckee@chem.auburn.edu.

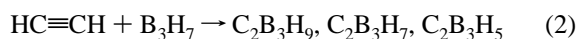
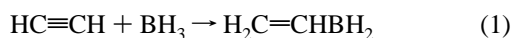
- (1) Grimes, R. N. *Carboranes*; Academic Press: New York, 1970.
- (2) Williams, R. E. *Chem. Rev.* **1992**, *92*, 177.
- (3) (a) Greatrex, R.; Fox, M. A. Reactions of Unsaturated Hydrocarbons with Small Boranes: New Insights and Recent Advances. In *The Borane, Carborane and Carbocation Continuum*; Casanova, J., Ed.; Wiley: New York, 1998; pp 289–305. (b) Berndt, A.; Hofmann, M.; Siebert, W.; Wrackmeyer, B. Carboranes: From Small Organoboranes to Clusters. In *Molecular Clusters of the Main Group Elements*; Driess, M., Nöth, H., Eds.; Wiley-VCH: Weinheim, 2004; pp 267–309.
- (4) Greatrex, R.; Greenwood, N. N.; Kirk, M. *Chem. Commun.* **1991**, 1510.
- (5) Fox, M. A.; Greatrex, R.; Greenwood, N. N.; Kirk, M. *Polyhedron* **1993**, *12*, 1849.
- (6) Fox, M. A.; Greatrex, R.; Hofmann, M.; Schleyer, P. v. R. *Angew. Chem., Int. Ed. Engl.* **1994**, *33*, 2298.
- (7) Köster, R.; Boese, R.; Wrackmeyer, B.; Schanz, H.-J. *J. Chem. Soc. Chem. Commun.* **1995**, 1691.
- (8) Wrackmeyer, B.; Schanz, H.-J. *Collect. Czech. Chem. Commun.* **1997**, *62*, 1253.
- (9) Williams, R. E.; Gerhart, F. J. *J. Organomet. Chem.* **1967**, *10*, 168.

- (10) Onak, T.; Gross, K.; Tse, J.; Howard, J. J. *J. Chem. Soc. Dalton* **1973**, 2633.
- (11) Brain, P. T.; Bühl, M.; Fox, M. A.; Greatrex, R.; Leuschner, E.; Picton, M. J.; Rankin, D. W. H.; Robertson, H. E. *Inorg. Chem.* **1995**, *34*, 2481.
- (12) Fox, M. A.; Greatrex, R.; Hofmann, M.; Schleyer, R. v. P.; Williams, E. R. *Angew. Chem., Int. Ed. Engl.* **1997**, *36*, 1498.
- (13) Fox, M. A.; Greatrex, R.; Nikrahi, A.; Brain, P. T.; Picton, M. J.; Rankin, D. W. H.; Robertson, H. E.; Bühl, M.; Li, L.; Beaudet, R. A. *Inorg. Chem.* **1998**, *37*, 2166.

Scheme 1

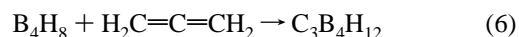
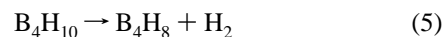
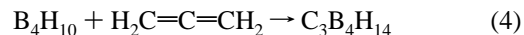
Reactants	Conditions	Observed Products	Reference
$B_4H_{10}$ + allene	Hot/Cold	2,4-(MeCHCH <sub>2</sub> )B <sub>4</sub> H <sub>8</sub> (1)	10
	70°C quenched	arachno-1,2-Me <sub>2</sub> -1-CB <sub>4</sub> H <sub>8</sub> (8) arachno-1,3-Me <sub>2</sub> -1-CB <sub>4</sub> H <sub>8</sub> (8a)	12
	70°C quenched loss of H <sub>2</sub>	1-Me-2,5-μ-CH <sub>2</sub> -1-CB <sub>4</sub> H <sub>7</sub> (29) 2,5-μ-CHMe-1-CB <sub>4</sub> H <sub>8</sub> (25/26)	12
$B_4H_{10}$ + methylacetylene	70°C quenched loss of H <sub>2</sub>	1-Me-2,5-μ-CH <sub>2</sub> -1-CB <sub>4</sub> H <sub>8</sub> (29) 2,5-μ-CHMe-1-CB <sub>4</sub> H <sub>8</sub> (25/26) (in 6:1 ratio)	5,6
	25-50°C loss of 2H <sub>2</sub>	2-Me-2,3-C <sub>2</sub> B <sub>4</sub> H <sub>7</sub> (34)	4

orbital on boron. Several mechanistic steps have been identified, the most notable of which is the diamond-square-diamond (DSD) step<sup>14,15</sup> where two fused diamonds go through a square transition state to form products with an interchange of bonds. Another well-known step is the hydroboration (HB) step in which an empty orbital on boron forms a  $\pi$  complex with a C–C double or triple bond followed by migration of the BH hydrogen to one carbon and the boron to the other carbon. It is known that acetylene adds to boron hydrides to form carboranes in which the C–C triple bond can be ultimately broken. How this is achieved is not completely understood, but theoretical calculations are making a contribution.<sup>16–21</sup> In a series of two papers,<sup>16,17</sup> one of the authors computed the reaction of acetylene with  $B_4H_{10}$  with the assumption that the first step of the reaction was the decomposition of  $B_4H_{10}$  to  $BH_3$ ,  $B_3H_7$ , and  $B_4H_8$  (eqs 1–3). In a subsequent paper<sup>18</sup> the addition of ethylene to  $B_4H_{10}$  was studied where a path to the basket 2,4-(CH<sub>2</sub>CH<sub>2</sub>)B<sub>4</sub>H<sub>8</sub> was identified.



The rate-determining step in the reaction of  $B_4H_{10}$  with many unsaturated hydrocarbons involves the elimination of H<sub>2</sub> to give  $B_4H_8$  as the reactive species (eq 5).<sup>22–26</sup>

- (14) Lipscomb, W. N. *Science* **1966**, *153*, 373.  
 (15) Mingos, D. M. P.; Johnston, R. L. *Polyhedron* **1988**, *7*, 2437.  
 (16) McKee, M. L. *J. Am. Chem. Soc.* **1995**, *117*, 8001.  
 (17) McKee, M. L. *J. Am. Chem. Soc.* **1996**, *118*, 421.  
 (18) Bühl, M.; McKee, M. L. *Inorg. Chem.* **1998**, *37*, 4953.  
 (19) McKee, M. L. *Inorg. Chem.* **2000**, *39*, 4206.  
 (20) Brown, C. A.; McKee, M. L. *J. Mol. Model.* **2006**, *12*, 653.  
 (21) McKee, M. L. Mechanistic Patterns in Carborane Reactions as Revealed by ab Initio Calculations. In *The Borane, Carborane and Carbocation Continuum*; Casanova, J., Ed.; Wiley: New York, 1998; pp 259–288.  
 (22) Greatrex, R.; Greenwood, N. N.; Potter, C. D. *J. Chem. Soc. Dalton Trans.* **1984**, 2435.  
 (23) Greatrex, R.; Greenwood, N. N.; Potter, C. D. *J. Chem. Soc. Dalton Trans.* **1986**, 81.  
 (24) Greenwood, N. N.; Greatrex, R. *Pure Appl. Chem.* **1987**, *59*, 857.  
 (25) Greenwood, N. N. *Electron Deficient Boron and Carbon Clusters*; Olah, G. A., Wade, K., Williams, R. E., Eds.; Wiley: New York, 1991; pp 165–181.



A study by Fox et al.<sup>12</sup> demonstrated that the formation of  $C_3B_4H_{14}$  according to eq 4 and the formation of  $C_3B_4H_{12}$  according to eqs 5 and 6 may be competitive with each other. The latter carborane,  $C_3B_4H_{12}$ , was first produced by Greatrex et al.<sup>4</sup> from the reaction between  $B_4H_{10}$  and propyne under hot/cold conditions. However, their proposed structure, based on NMR evidence, was subsequently shown by Fox et al.<sup>5</sup> to be incorrect.

## Methods

Since the MP2/6-31G(d) method has provided accurate geometries for boranes and carboranes,<sup>27</sup> all geometries were fully optimized at the MP2/6-31G(d) level. Vibrational frequencies were calculated at that level to make zero-point energy and thermal corrections and single-point calculations were made at the CCSD(T)/6-311+G(d) level to give more reliable energies. All electronic structure calculations have used the Gaussian 03 program.<sup>28</sup> Imaginary frequencies for transition states were animated by using graphical program MolDen<sup>29</sup> to ensure that the motion of the transition vector was appropriate for converting reactants to products. In addition, intrinsic reaction coordinate (IRC) calculations have been performed on most transition states to verify which minima are connected to the transition state. In the discussion below, all free energies denoted by  $\Delta G$  at 298 K are relative to  $B_4H_{10}$  plus allene while free energies of activation denoted by  $\Delta G^\ddagger$  at 298 K are relative to an individual reaction step.

## Results and Discussions

In the reaction of  $B_4H_{10}$  with allene, some of the observed products do not involve the initial loss of H<sub>2</sub>. We considered two initial hydroboration steps (Figures 1 and 2), one from  $B_4H_{10}$  ( $2 \rightarrow TS2/3 \rightarrow 3$ ), and another involving an activated form of  $B_4H_{10}$  ( $2 \rightarrow TS2/2a \rightarrow 2a \rightarrow TS2a/3 \rightarrow 3$ ). The activated form of  $B_4H_{10}$  has a five-coordinate boron center (**2a**) and has been implicated in the initial hydroboration step of  $B_4H_{10}$

- (26) Nöth, H. Mononuclear Boron Cluster. In *Molecular Clusters of the Main Group Elements*; Driess, M., Nöth, H., Eds.; Wiley-VCH: Weinheim, 2004; pp 34–94.  
 (27) Bühl, M.; Schleyer, P. v. R. *J. Am. Chem. Soc.* **1992**, *114*, 477.  
 (28) Frisch, M. J.; Trucks, G. W.; Schlegel, H. B.; Scuseria, G. E.; Robb, M. A.; Cheeseman, J. R.; Montgomery, J. A., Jr.; Vreven, T.; Kudin, K. N.; Burant, J. C.; Millam, J. M.; Iyengar, S. S.; Tomasi, J.; Barone, V.; Mennucci, B.; Cossi, M.; Scalmani, G.; Rega, N.; Petersson, G. A.; Nakatsuji, H.; Hada, M.; Ehara, M.; Toyota, K.; Fukuda, R.; Hasegawa, J.; Ishida, M.; Nakajima, T.; Honda, Y.; Kitao, O.; Nakai, H.; Klene, M.; Li, X.; Knox, J. E.; Hratchian, H. P.; Cross, J. B.; Bakken, V.; Adamo, C.; Jaramillo, J.; Gomperts, R.; Stratmann, R. E.; Yazyev, O.; Austin, A. J.; Cammi, R.; Pomelli, C.; Ochterski, J. W.; Ayala, P. Y.; Morokuma, K.; Voth, G. A.; Salvador, P.; Dannenberg, J. J.; Zakrzewski, V. G.; Dapprich, S.; Daniels, A. D.; Strain, M. C.; Farkas, O.; Malick, D. K.; Rabuck, A. D.; Raghavachari, K.; Foresman, J. B.; Ortiz, J. V.; Cui, Q.; Baboul, A. G.; Clifford, S.; Cioslowski, J.; Stefanov, B. B.; Liu, G.; Liashenko, A.; Piskorz, P.; Komaromi, I.; Martin, R. L.; Fox, D. J.; Keith, T.; Al-Laham, M. A.; Peng, C. Y.; Nanayakkara, A.; Challacombe, M.; Gill, P. M. W.; Johnson, B.; Chen, W.; Wong, M. W.; Gonzalez, C.; Pople, J. A. *Gaussian 03*, revision D.01; Gaussian, Inc.: Wallingford, CT, 2004.  
 (29) Schaftenaar, G.; Noordik, J. H. *J. Comput.-Aided Mol. Design* **2000**, *14*, 123.

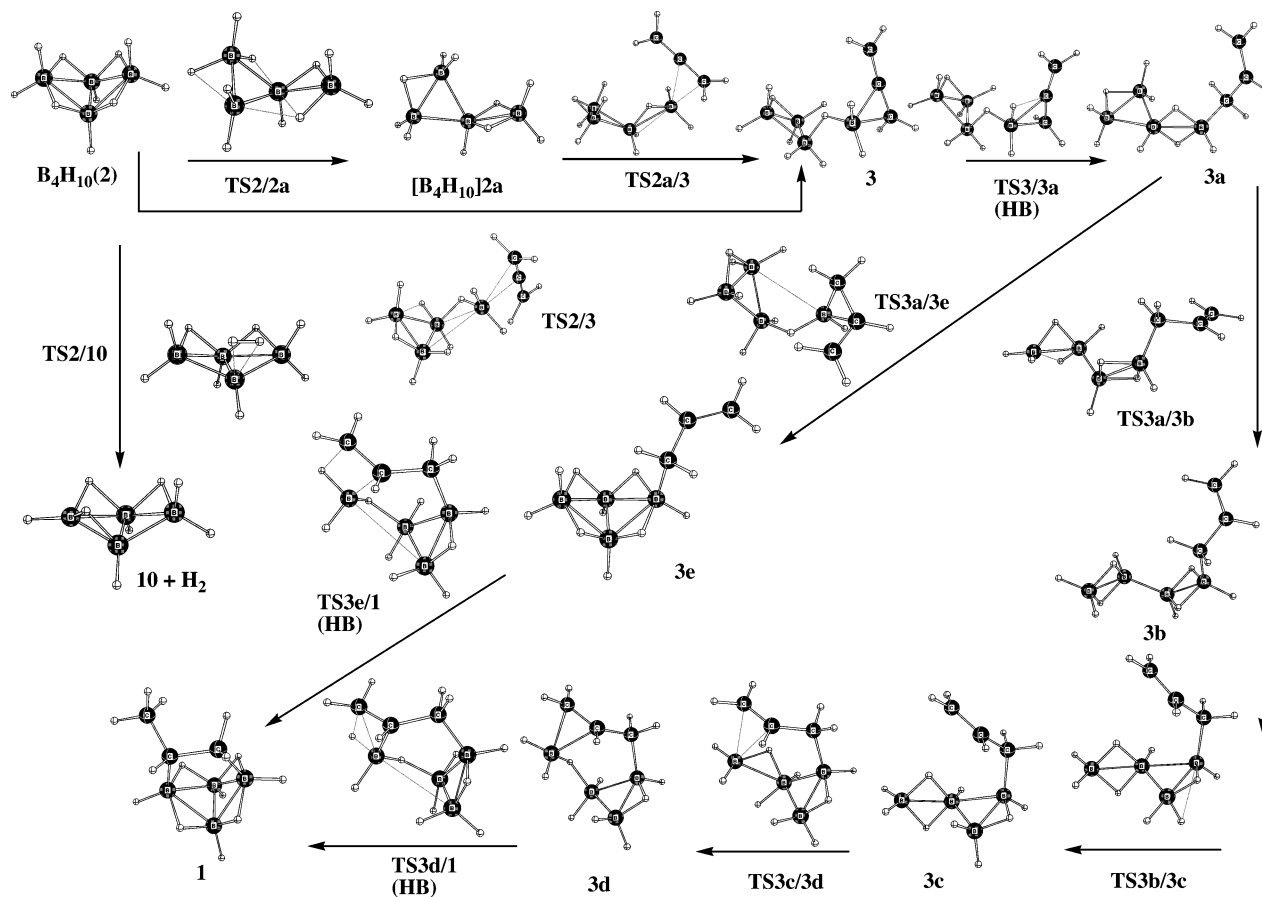


**Figure 1.** Stationary points along the reaction pathway for formation of basket compound **1**, MP2/6-31G(d) optimized. “HB” indicates a hydrobortion transition state.

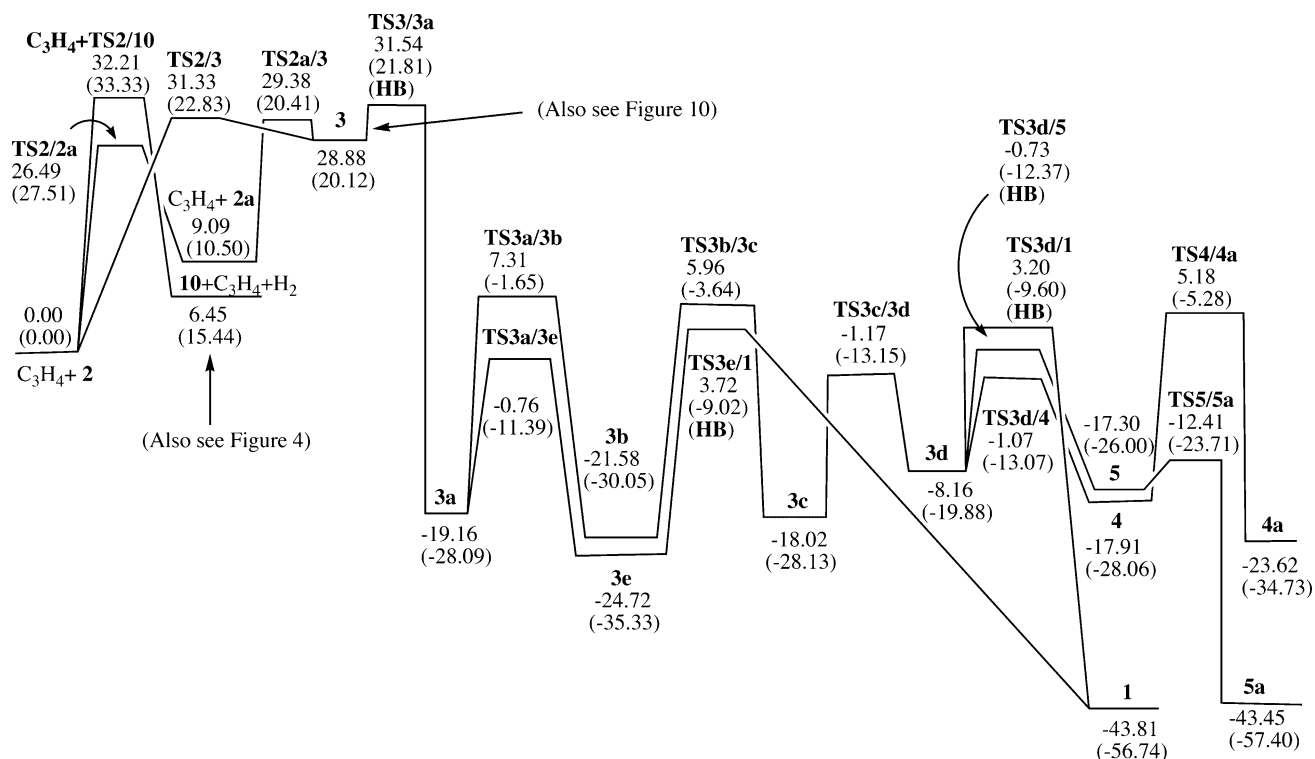


**Figure 2.** Schematic reaction profile for reaction of  $B_4H_8$  with allene at the CCSD(T)/6-311+G(d)//MP2/6-31G(d) level. Relative free energies (enthalpies) are given in kcal/mol at 298 K relative to allene +  $B_4H_{10}$ .

**Table 1.** Relative Energies, Enthalpies, and Free Energies (kcal/mol) of Various Species

	relative $\Delta H(298\text{ K})^a$		relative $\Delta G(298\text{ K})^a$
	CCSD(T)/b//		CCSD(T)/b//
	MP2/a	MP2/a	MP2/a
allene + B <sub>4</sub> H <sub>10</sub> ( <b>2</b> )	0.00	0.00	0.00
allene + <b>TS2/2a</b>	31.37	27.51	26.49
allene + <b>2a</b>	12.83	10.50	9.09
<b>TS2/10</b>	40.46	33.33	32.21
B <sub>4</sub> H <sub>8</sub> ( <b>10</b> ) + C <sub>3</sub> H <sub>4</sub> +H <sub>2</sub>	16.64	15.44	6.45
<b>TS2/3</b>	24.90	22.83	31.33
<b>TS2a/3</b>	21.74	20.41	29.38
<b>3</b>	20.95	20.12	28.88
<b>TS3/3a</b>	21.71	21.81	31.54
<b>3a</b>	-27.21	-28.10	-19.16
<b>TS3a/3e</b>	-11.80	-11.39	-0.76
<b>3e</b>	-37.19	-35.33	-24.72
<b>TS3e/1</b>	-16.82	-9.02	3.72
<b>TS3a/3b</b>	0.73	-1.65	7.31
<b>3b</b>	-28.91	-30.05	-21.58
<b>TS3b/3c</b>	-1.83	-3.64	5.96
<b>3c</b>	-27.94	-28.13	-18.02
<b>TS3c/3d</b>	-13.81	-13.15	-1.17
<b>3d</b>	-20.84	-19.88	-8.16
<b>TS3d/1</b>	-12.41	-9.60	3.20
<b>1</b>	-60.19	-56.74	-43.81
<b>TS3d/4</b>	-13.73	-13.07	-1.07
<b>4</b>	-27.87	-28.06	-17.91
<b>TS4/4a</b>	-3.76	-5.28	5.18
<b>4a</b>	-36.75	-34.73	-23.62
<b>TS3d/5</b>	-13.68	-12.37	-0.73
<b>5</b>	-26.83	-26.00	-17.30
<b>TS5/5a</b>	-23.36	-23.71	-12.41
<b>5a</b>	-61.26	-57.40	-43.45
<b>TS3/6</b>	25.18	24.76	34.34
<b>6</b>	-28.88	-28.58	-19.00
<b>TS6/12</b>	-10.28	-11.22	-0.84
<b>12</b>	-40.38	-37.60	-26.75
<b>TS6/6a</b>	-8.63	-9.46	1.94
<b>6a</b>	-17.93	-17.80	-6.22
<b>TS6a/7</b>	-12.37	-11.10	0.78
<b>7</b>	-52.23	-51.97	-39.42
<b>TS7/7a</b>	-19.61	-20.47	-8.51
<b>7a</b>	-32.58	-29.61	-17.58
<b>TS7a/8</b>	-1.44	1.25	14.04
1,2-Me <sub>2</sub> -1-CB <sub>4</sub> H <sub>8</sub> ( <b>8</b> )	-72.05	-65.50	-54.04
<b>TS8/8a</b>	-65.58	-59.97	-48.38
1,2-Me <sub>2</sub> -1-CB <sub>4</sub> H <sub>8</sub> ( <b>8a</b> )	-73.77	-67.48	-55.97

<sup>a</sup> Basis set "a" is 6-31G(d); basis set "b" is 6-311+G(d).

with ethylene<sup>18</sup> and in the butterfly to bisboranyl rearrangement in B<sub>4</sub>H<sub>10</sub>.<sup>30</sup> The two transition states, **TS2/3** and **TS2a/3**, resemble each other very strongly with the latter slightly lower in free energy (31.3 vs 29.4 kcal/mol). Both steps converge at structure **3** which has a small free energy barrier ( $\Delta G^\ddagger = 2.7$  kcal/mol) to form **3a**, a propene-substituted version of **2a**. Structure **3a** leads to the basket structure **1** in either two steps (**3a**→**3e**→**1**) or four steps (**3a**→**3b**→**3c**→**3d**→**1**). The highest intervening barrier in the two-step path is **TS3e/1** ( $\Delta G = 3.7$  kcal/mol), while it is **TS3a/3b** ( $\Delta G = 7.3$  kcal/mol) in the four-step path. We note that **3b** is a derivative of the bis(diboranyl) structure of B<sub>4</sub>H<sub>10</sub>.<sup>30,31</sup>

The initial hydroboration steps (Figures 1 and 2; **2**→**TS2/2a**→**2a**→**TS2a/3**→**3**→**TS3/3a**→**3a**) compete with the H<sub>2</sub> elimination step (**2**→**TS2/10**→**10**+H<sub>2</sub>); the former has a free energy of 31.5 kcal/mol (**TS3/3a**) and the latter 32.2 kcal/

**Table 2.** Relative Enthalpies and Free Energies (kcal/mol) of Various Species

	relative $\Delta H(298\text{ K})^a$		relative $\Delta G(298\text{ K})^a$
	CCSD(T)/b//		CCSD(T)/b//
	MP2/a	MP2/a	MP2/a
allene + B <sub>4</sub> H <sub>8</sub> ( <b>10</b> )	16.64	15.44	6.45
<b>TS10/11</b>	26.24	24.61	25.91
<b>11</b>	-5.69	1.34	4.42
<b>TS11/12</b>	23.54	31.72	35.09
<b>12</b>	-43.81	-34.99	-31.20
<b>TS12/13</b>	-26.01	-19.24	-14.87
<b>13</b>	-39.54	-33.53	-29.31
<b>TS13/14</b>	-13.84	-11.62	-7.41
<b>14</b>	-14.19	-11.33	-7.51
<b>TS14/15</b>	-0.88	2.79	7.24
<b>15</b>	-9.11	-5.21	-1.33
<b>TS15/16</b>	-0.14	3.11	7.27
<b>16</b>	-10.52	-6.85	-3.06
<b>TS16/17</b>	-9.59	-7.08	-3.12
<b>17</b>	-26.47	-21.95	-18.50
<b>TS17/18</b>	-4.87	-0.61	2.81
<b>18</b>	-23.99	-18.38	-15.43
<b>TS18/19</b>	-22.08	-17.95	-14.72
<b>19</b>	-28.84	-25.50	-22.59
<b>TS19/20</b>	-21.19	-17.36	-14.39
<b>20</b>	-31.99	-25.50	-22.25
<b>TS20/21</b>	-15.08	-8.47	-4.78
<b>21</b>	-31.79	-25.87	-22.50
<b>TS21/22</b>	-29.50	-23.04	-19.05
<b>22</b>	-42.81	-35.31	-31.15
<b>TS22/23</b>	-23.40	-16.69	-12.31
<b>23</b>	-26.07	-21.60	-17.43
<b>TS23/24</b>	-5.99	-2.72	1.22
<b>24</b>	-11.39	-3.91	-0.89
<b>TS24/25</b>	-2.42	6.61	10.63
<b>25</b>	-61.39	-53.41	-49.06
<b>TS25/26</b>	-13.15	-5.40	-2.82
<b>26</b>	-60.69	-52.58	-48.33
<b>TS13/27</b>	-3.20	-3.99	0.06
<b>27</b>	-34.74	-32.14	-28.69
<b>TS27/28</b>	-27.57	-23.79	-20.80
<b>28</b>	-42.79	-39.99	-37.96
<b>TS28/29</b>	-25.16	-21.80	-18.82
<b>29</b>	-63.64	-55.30	-51.27
<b>TS13/30</b>	16.63	18.39	21.47
<b>30</b>	-1.97	4.21	-1.07
<b>TS30/31</b>	13.39	16.08	10.41
<b>31</b>	7.40	9.95	3.62
<b>TS31/32</b>	8.59	10.90	5.05
<b>32</b>	6.50	11.95	5.66
<b>TS32/33</b>	5.83	11.39	6.06
<b>33</b>	-39.93	-29.48	-33.87
<b>TS33/34</b>	-38.86	-27.48	-31.92
<b>34</b>	-64.22	-52.49	-56.82

<sup>a</sup> Basis set "a" is 6-31G(d); basis set "b" is 6-311+G(d).

mol (**TS2/10**). The B<sub>4</sub>H<sub>8</sub> species **10** with three BHB bridges adds to a double bond of allene to form **11**, followed by a hydroboration step (Figures 3 and 4; **TS11/12**). The activation free energy for this step is high ( $\Delta G^\ddagger = 30.7$  kcal/mol). A pentagonal pyramid (**13**) is formed next with adjacent carbons in the base, much like the framework of the well-known 2,3-C<sub>2</sub>B<sub>4</sub>H<sub>8</sub> isomer.<sup>32</sup> This intermediate will serve as the starting point (Figures 5 and 6) for formation of 2-Me-2,3-C<sub>2</sub>B<sub>4</sub>H<sub>7</sub> (**34**), a product observed<sup>4</sup> in the reaction of methylacetylene with B<sub>4</sub>H<sub>10</sub>, but not in the reaction of allene with B<sub>4</sub>H<sub>10</sub>.<sup>12</sup>

(30) Ramakrishna, V.; Duke, J. B. *Inorg. Chem.* **2004**, *43*, 8176.

(31) McKee, M. L. *Inorg. Chem.* **1986**, *25*, 3545.

(32) Hofmann, M.; Fox, M. A.; Greatrex, R.; Williams, R. E.; Schleyer, P. v. R. *J. Organomet. Chem.* **1998**, *550*, 331.

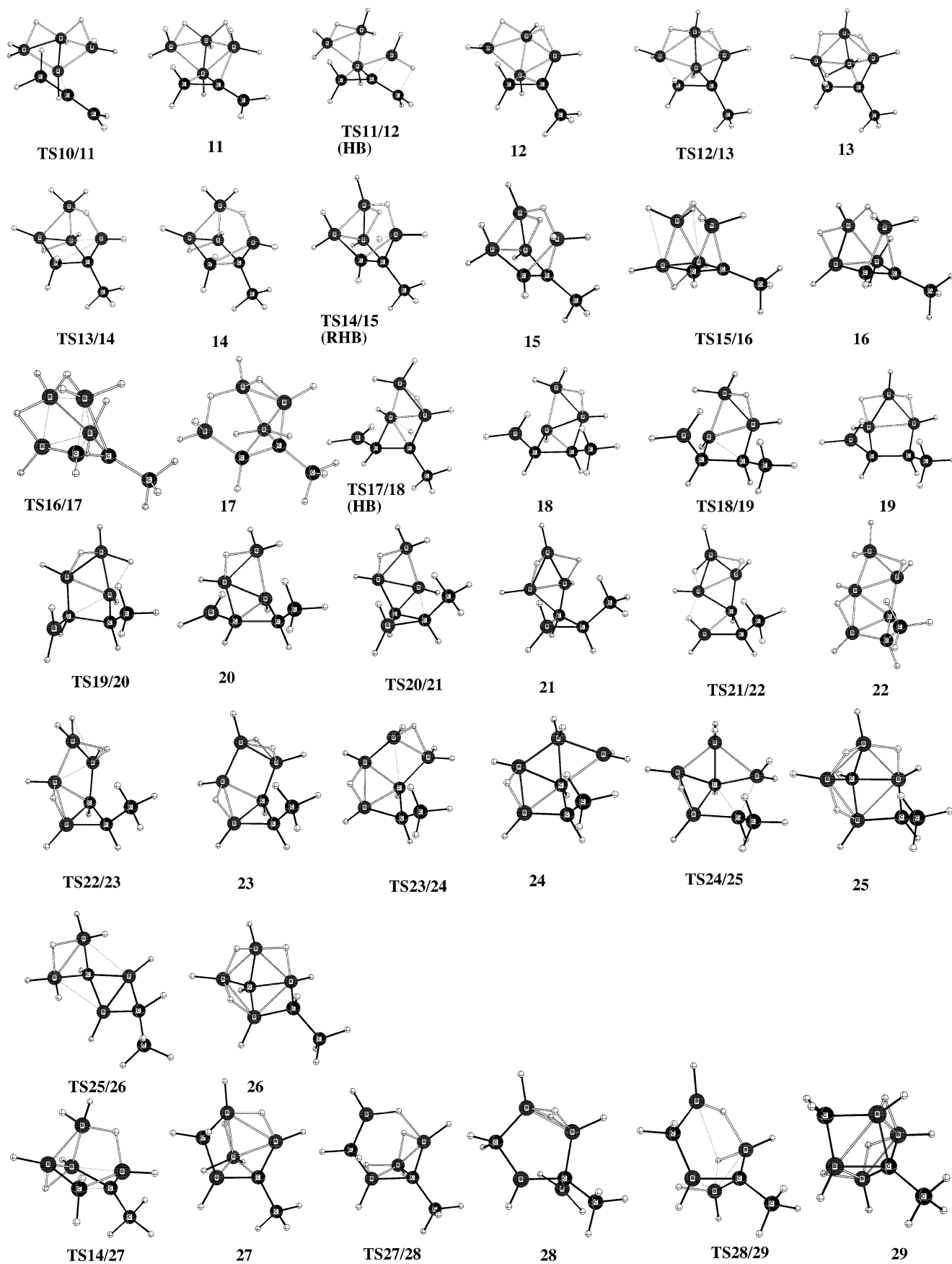
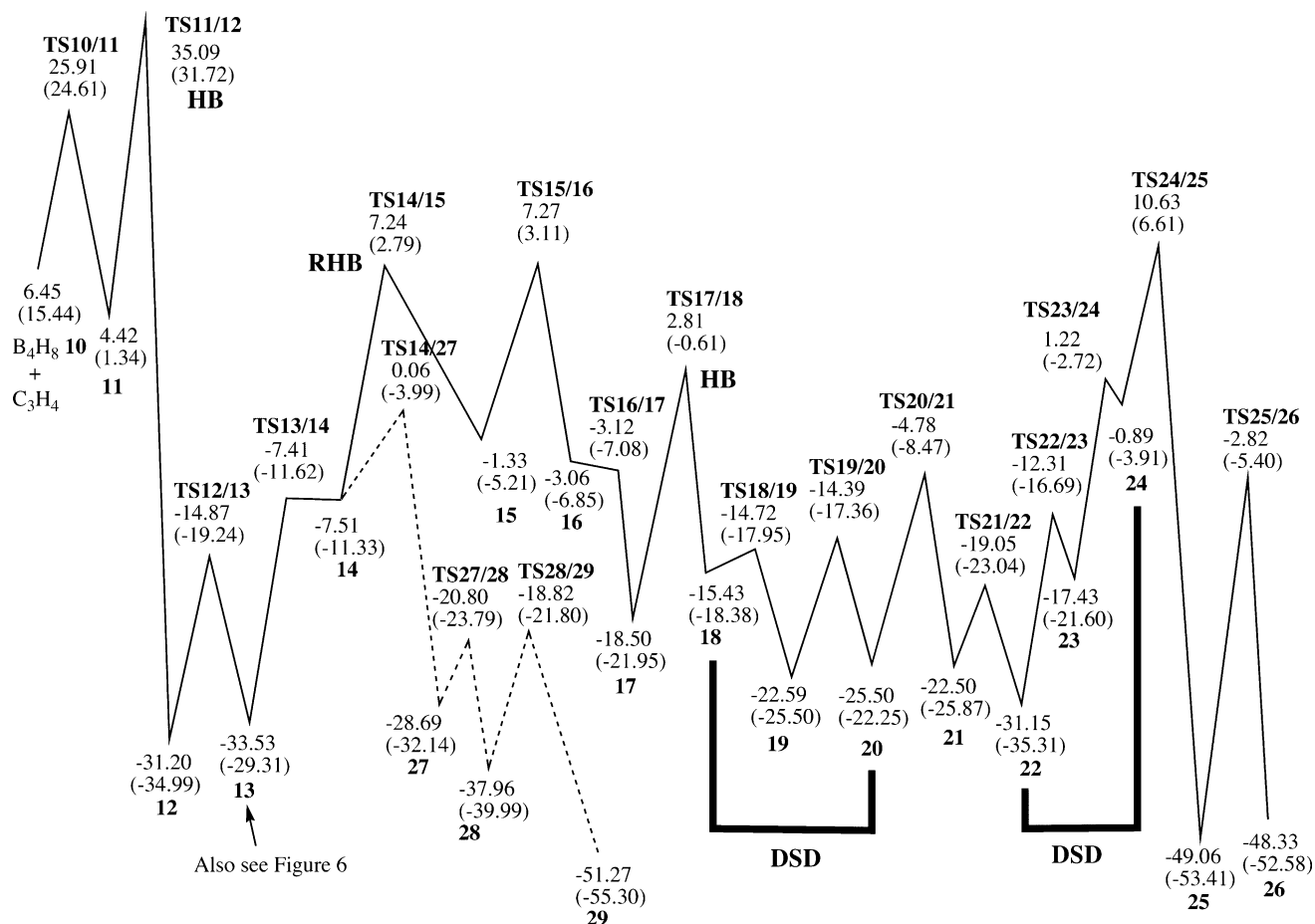
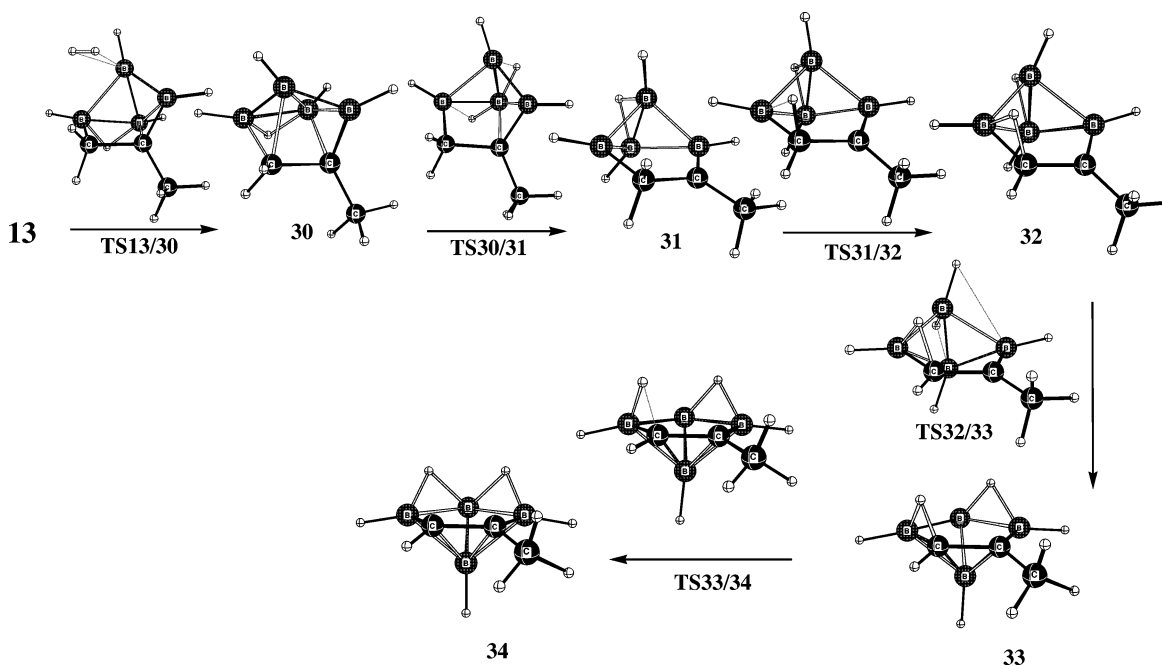


Figure 3. Stationary points along for the formation of *arachno*-carbapentaborane (25/26 and 29), MP2/6-31G(d) optimized.



**Figure 4.** Schematic reaction profile for formation of **25/26** and **29** at the CCSD(T)/6-311+G(d)/MP2/6-31G(d) level. Relative free energies (enthalpies in parentheses) are given in kcal/mol at 298 K relative to allene +  $B_4H_{10}$ . All intermediates and transition states contain a  $H_2$  molecule.



**Figure 5.** Stationary points along for the formation of 2-Me-2,3- $C_2B_4H_7$  (**34**), MP2/6-31G(d) optimized.

The reaction of **13**→[**TS13/14**→**14**]<sup>33</sup>→**TS14/15**→**15** (Figure 4;  $\Delta G^\ddagger = 40.8$  kcal/mol) is an example of a reverse hydroboration (RHB) step where a CH hydrogen is transferred to boron. The reaction **15**→**TS15/16**→**16** is a syn-

chronous conversion of a BHB→BH and a BH→BHB involving two hydrogen atoms. In the next step, **16**→**TS16/17**→**17**, substantial rearrangement occurs with almost no activation. Another hydroboration (HB) step occurs in

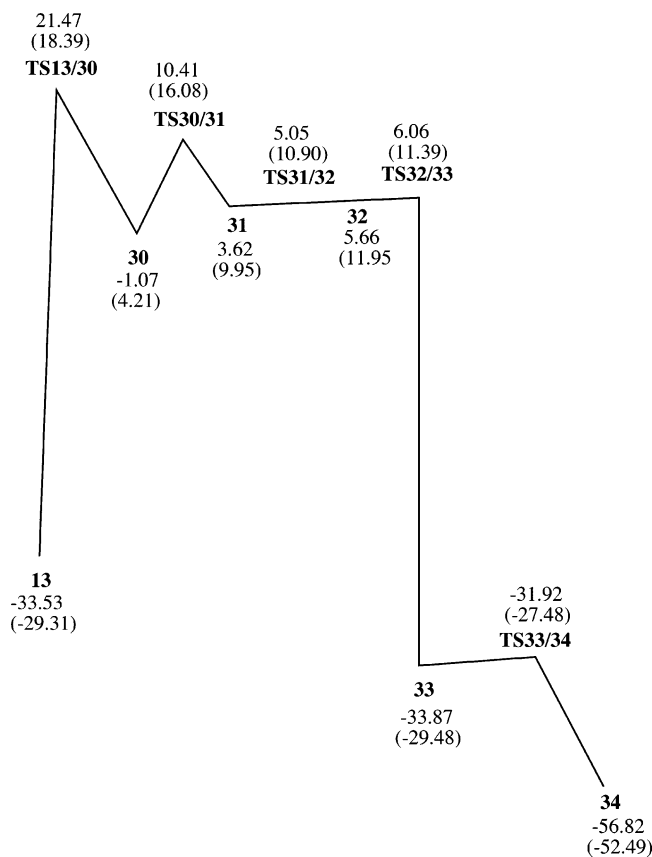


**Figure 6.** Schematic reaction profile for formation of **34** at the CCSD(T)/6-311+G(d)/MP2/6-31G(d) level. Relative free energies (enthalpies in parentheses) are given in kcal/mol at 298 K relative to allene +  $B_4H_{10}$ . All intermediates and transition states contains two  $H_2$  molecules except **13** and **TS13/30** which have one  $H_2$  molecule.

**17**→**TS17/18**→**18** with  $\Delta G^\ddagger = 21.3$  kcal/mol to produce an intermediate **18** with an external  $BH_2$  group. In the reaction sequence **18**→**TS18/19**→**19**→**TS19/20**→**20**, a DSD step takes place in the  $C_2B_2$  unit. In the **20**→**TS20/21**→**21** step, a B–C bond is created, while in the **21**→**TS21/22**→**22** step, the external  $BH_2$  group is incorporated into the cluster. From **22** to **24**, another DSD step takes place in a  $CB_3$  unit to form an unstable intermediate **24**.<sup>34</sup> The critical C–C bond breaking process **24**→**TS24/25**→**25** is compensated by the formation of a C–B bond to form *endo*-2,5- $\mu$ -CHMe-1- $CB_4H_8$  (**25**). There is ambiguity on the orientation of the methyl group in 2,5- $\mu$ -CHMe-1- $CB_4H_8$ .<sup>3a,6,12</sup> In ref 6, the methyl group is indicated as *endo* (**25**), while in refs 3a and 12, the product is indicated as *exo* (**26**). The present calculations would suggest that the observed product is **25** rather than **26** because there is a very high free energy barrier of  $\Delta G^\ddagger = 46.2$  kcal/mol between the two isomers.

The reaction path to form 1-Me-2,5- $\mu$ - $CH_2$ -1- $CB_4H_7$  (**29**) starts at **14** by breaking a C–C bond to form **27** (Figures 3 and 4). From **27** to **28**, a terminal  $BH_2$  group is created which is incorporated into the cluster when **29** is formed. Structure

(33) The brackets are used in the reaction sequence to indicate that the transition state **TS13/14** is lower in energy than the intermediate **14**, which suggests that the actual reaction is **13**→**TS14/15**→**15**.

(34) A second pathway from **22**→**25** was located (not shown) with a  $BH_2$  group pivot which had a free energy lower by 0.6 kcal/mol.

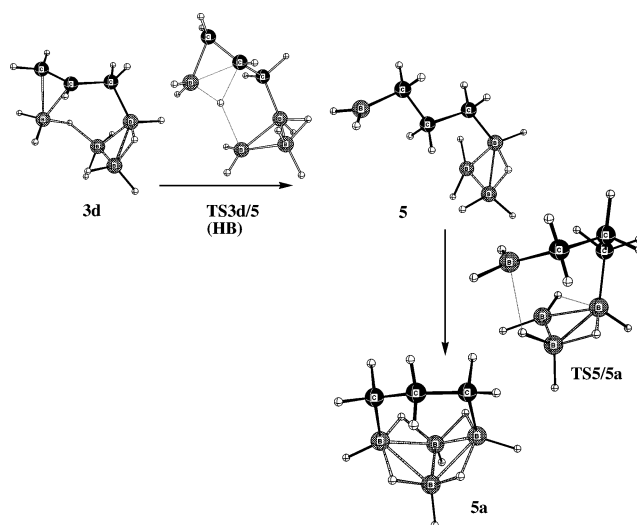


**Figure 7.** Stationary points for the formation of basket compound **5a**.

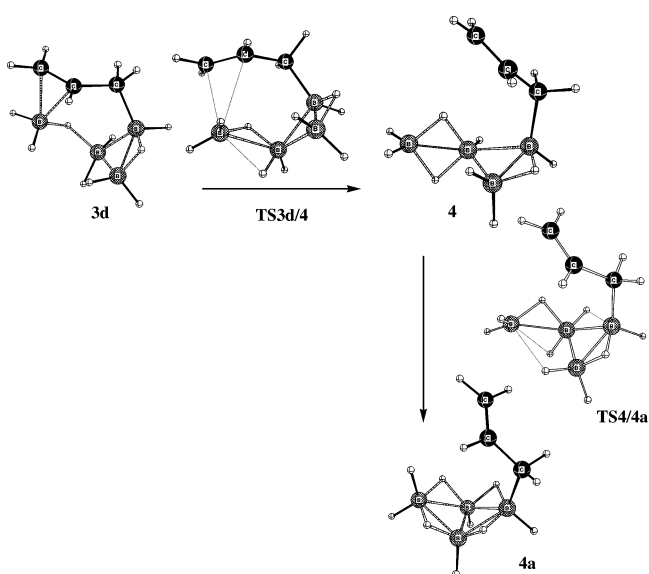


**Figure 8.** Stationary points for formation of allyl-substituted tetraborane **4a**.

**29** is one of the dominant species formed in the reaction between allene and  $B_4H_{10}$ .

Starting at structure **13** (Figures 5 and 6) a reaction path was followed for the formation of 2-Me-2,3- $C_2B_4H_7$  (**34**). It would appear that loss of  $H_2$  from **13** would lead to **34**, and indeed it does. However, the  $H_2$ -elimination step was computed to have a much higher free energy of activation (**13**→**TS13/30**→**30**  $\Delta G^\ddagger = 55.0$  kcal/mol) than other steps. From the intermediate **30**, four steps with small free energy barriers (**30**→**31**→**32**→**33**→**34**) lead to the global minimum. Thus, **34** is not formed in the reaction due to the higher barrier for  $H_2$  loss (**13**→**TS13/30**→**30**). In the reaction between acetylene and  $B_4H_8$ , a  $C_2B_4H_{10}$  product is formed which has a relatively low barrier for loss of  $H_2$  to give 2,3- $C_2B_4H_8$  (a demethylated version of **34**) directly. This same reaction pathway would be available for methylacetylene and would lead to 2-Me-2,3- $C_2B_4H_7$  (**34**), but would not be available to allene due to the absence of a C–C triple bond.

An example of intramolecular hydroboration is given by **3d**→**TS3d/5**→**5** (Figures 1 and 7) in which the transition

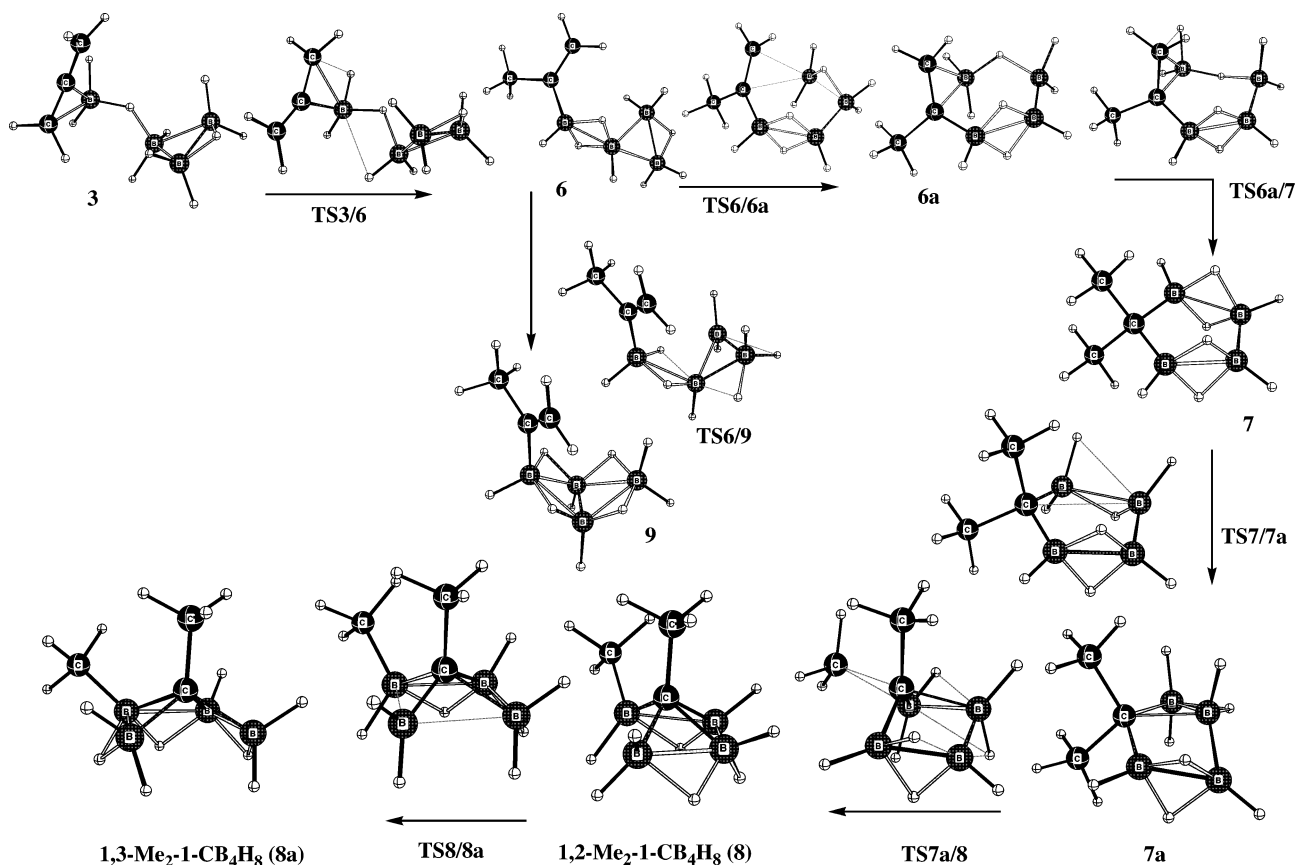


**Figure 9.** Stationary points along for the formation of *arachno*-1,3- (**8a**) and *arachno*-1,2-Me<sub>2</sub>-1-CB<sub>4</sub>H<sub>8</sub> (**8**), MP2/6-31G(d) optimized.

state is stabilized by the interaction of the transferring hydrogen with an empty orbital on the B<sub>3</sub>H<sub>7</sub>-like unit.<sup>18</sup> The product **5**, a derivative of B<sub>3</sub>H<sub>7</sub> with a BH<sub>2</sub>-CH<sub>2</sub>-CH<sub>2</sub>-CH<sub>2</sub> group, can add the tethered BH<sub>2</sub> to the B<sub>3</sub>H<sub>7</sub>-like fragment to form **5a**, a 2,4-(CH<sub>2</sub>CH<sub>2</sub>CH<sub>2</sub>)B<sub>4</sub>H<sub>8</sub> basket, with a free energy of -43.4 kcal/mol. The reaction step (**5**→**TS5/5a**→**5a**) is very similar to a related step in the reaction of B<sub>4</sub>H<sub>10</sub> + C<sub>2</sub>H<sub>4</sub> where the BH<sub>2</sub> end of a tethered BH<sub>2</sub>-CH<sub>2</sub>-CH<sub>2</sub> group adds to the B<sub>3</sub>H<sub>7</sub>-like unit to form a 2,4-(CH<sub>2</sub>CH<sub>2</sub>)B<sub>4</sub>H<sub>8</sub> basket.<sup>18</sup> Both reaction steps are directly analogous to the intermolecular reaction B<sub>3</sub>H<sub>7</sub> + BH<sub>3</sub> → B<sub>4</sub>H<sub>10</sub> where a terminal hydrogen of the BH<sub>2</sub> group forms a bridging interaction while at the same time the empty p orbital of the BH<sub>2</sub> interacts with a terminal hydrogen in B<sub>3</sub>H<sub>7</sub>.<sup>16</sup>

Intermediate **3d** can form **4** via the transition state **TS3d/4** where two C-B bonds are broken while a terminal BH bond becomes bridging (Figures 1 and 8). Intermediate **4**, a propenyl-substituted version of **2a**, can form **4a**, a propenyl-substituted tetraborane and a different conformation of **3e**, over a moderate free energy barrier ( $\Delta G^\ddagger = 23.1$  kcal/mol). The reverse reaction step (**4a**→**TS4/4a**→**4**) is analogous to the **2**→**TS2/2a**→**2a** reaction where a five-coordinate-boron B<sub>4</sub>H<sub>10</sub> intermediate is formed. In both reactions, a relatively stable species (**4a** and **2**) is converted into a much more reactive intermediate (**4** and **2a**) with free energy barriers of  $\Delta G^\ddagger = 28.8$  and 26.5 kcal/mol, respectively. The five-coordinate boron is also observed in the structures of **3a** and **6**.

The potential energy surface (Figure 2) shows that there is a competition in formation of basket compounds **1** and **5a**. Even though **1** and **5a** have similar free energies (-43.8 and -43.4 kcal/mol, respectively), **5a** was not observed in the Onak study.<sup>10</sup> This is consistent with the highest transition state free energy in the process **3a**→**3e**→**1** (**TS3e/1**, 3.7 kcal/mol) which is 3.6 kcal/mol lower than the highest transition state free energy in the process **3a**→**3b**→**3c**→**3d**→**5**→**5a** (**TS3a/3b**, 7.3 kcal/mol).

Monocarborapentaborane isomers *arachno*-1,3- (**8a**) and *arachno*-1,2-Me<sub>2</sub>-1-CB<sub>4</sub>H<sub>8</sub> (**8**) are synthesized from the quenched reaction of B<sub>4</sub>H<sub>10</sub> with allene in the study by Fox et al.<sup>12</sup> The route from the high-energy intermediate **3** proceeds to **6** with an activation free energy of  $\Delta G^\ddagger = 5.5$  kcal/mol (**TS3/6**, Figures 9 and 10). From intermediate **6** there are two pathways, one leads to *arachno* isomers **8** and **8a** starting with transition state **TS6/6a** ( $\Delta G^\ddagger = 20.9$  kcal/mol higher than **6**) and the other forms a propene-substituted borane **9** via transition state **TS6/9** ( $\Delta G^\ddagger = 18.2$  kcal/mol higher than **6**).

Breaking a B-B bond and forming two C-B bonds in **TS6/6a** leads to **6a** that is 6.2 kcal/mol lower in free energy than B<sub>4</sub>H<sub>10</sub> + allene. The reaction **6a**→**TS6a/7**→**7** is a hydroboration step with a modest barrier of  $\Delta G^\ddagger = 7.0$  kcal/mol to form **7**. The intermediate 2,4-CMe<sub>2</sub>-bisdiborane (**7**) has C<sub>2v</sub> symmetry and is 39.4 kcal/mol lower in free energy than B<sub>4</sub>H<sub>10</sub> + allene. While structure **7** has not yet been reported, it lies in a rather deep free energy well with free



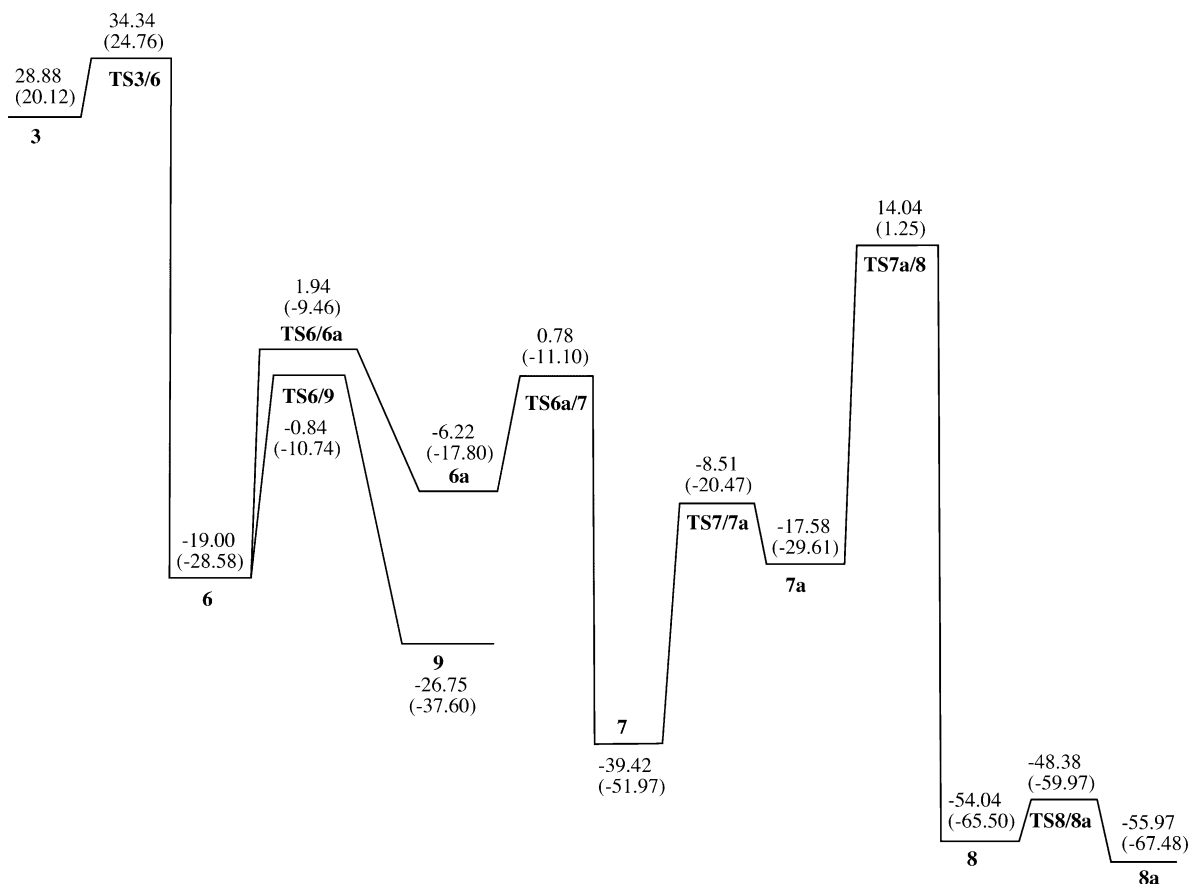


**Figure 10.** Schematic reaction profile for formation of *arachno*-1,3- (**8a**) and *arachno*-1,2-Me<sub>2</sub>-1-CB<sub>4</sub>H<sub>8</sub> (**8**) at the CCSD(T)/6-311+G(d)//MP2/6-31G(d) level. Relative free energies (enthalpies in parentheses) are given in kcal/mol at 298 K relative to allene plus B<sub>4</sub>H<sub>10</sub>.

energy barriers of  $\Delta G^\ddagger = 40.2$  (**7**→**6a**) and 53.5 kcal/mol (**7**→**8**).

The transition state **TS7/7a** was located for the transformation of **7** into **7a** where a BH bridge bond is converted into BH terminal bond. The next step is the migration of a methyl group from carbon to boron (**7a**→**TS7a/8**→**8**) with a free energy barrier of  $\Delta G^\ddagger = 31.6$  kcal/mol to form *arachno*-1,2-Me<sub>2</sub>-1-CB<sub>4</sub>H<sub>8</sub> (**8**). Fox et al. assumed that there was a rapid equilibrium between **8** and **8a** with isomer **8a** lower in energy than **8**. Our potential energy surface showed that **8** can easily convert to **8a** through free energy barrier of  $\Delta G^\ddagger = 5.7$  kcal/mol ( $\Delta H^\ddagger = 5.5$  kcal/mol). Fox et al.<sup>12</sup> calculated a similar activation barrier for **8**→**TS8/8a**→**8a** ( $\Delta H^\ddagger = 7.5$  kcal/mol) with a reaction enthalpy of  $-1.7$  kcal/mol which can be compared to our value of  $\Delta H_{rxn} = -2.0$  kcal/mol.

## Conclusion

The complicated mechanism of carborane formation from boron hydrides plus allene (B<sub>4</sub>H<sub>10</sub> + C<sub>3</sub>H<sub>4</sub>) have been studied

computationally. A new basketlike compound **5a** is found which is only slightly less stable than the observed basket **1**. The potential energy surface shows that there is competition for the production of **1** and **5a** and also for the production of *arachno*-1,3- (**8a**) and *arachno*-1,2-Me<sub>2</sub>-1-CB<sub>4</sub>H<sub>8</sub> (**8**). The production of *arachno*-carbapentaboranes (**25/26** and **29**) is less favorable due to a higher free energy of activation barrier for loss of H<sub>2</sub> from B<sub>4</sub>H<sub>10</sub> relative to allene addition.

**Acknowledgment.** Computer time was made available on the Alabama Supercomputer Network.

**Supporting Information Available:** MP2/6-31G(d) and CCSD(T)/6-311+G(d) energies (hartrees), zero-point energies (kcal/mol), heat capacity corrections to 298 K (kcal/mol), entropies (cal/mol·K) at the MP2/6-31G(d) level are tabulated in Table S1 and Table S2. Cartesian coordinates of all optimized structures at the MP2/6-31G(d) level are given in Table S3. This material is available free of charge via the Internet at <http://pubs.acs.org>.

IC070076X